

A COMBINED APPROACH OF NUMERICAL SIMULATION AND ADDITIVE MANUFACTURING TECHNIQUE FOR IN-SILICO AND IN-VITRO TESTING OF A 3D PRINTING-BASED AORTIC POLYMERIC HEART VALVE

E. Gasparotti^{*†}, U. Cella[‡], E. Vignali^{*†}, E. Costa^{††}, G. Soldani^{**}, A. Cavallo^{**}, P. Losi^{**},
M.E. Biancolini[‡] and S. Celi^{*}

^{*} BioCardioLab, Fondazione Toscana "G. Monasterio",
Heart Hospital, Via Aurelia Sud, 54100 Massa
e-mail: gasparotti@ftgm.it, evignali@ftgm.it, s.celi@ftgm.it web page: bcl.ftgm.it

[†] Department of Information Engineering, University of Pisa, Italy
Via G. Caruso 16 - 56122 - Pisa

^{**} Biomaterials and regenerative medicine, Clinical Physiology Institute CNR
Heart Hospital, Via Aurelia Sud, 54100 Massa
aida.cavallo@ifc.cnr.it, giorgio.soldani@ifc.cnr.it, losi@ifc.cnr.it

^{††} RINA Consulting S.p.A.
Viale Cesare Pavese, 305 - 00144, Roma, Italy
emiliano.costa@rina.org

[‡] Department of Enterprise Engineering Mario Lucertini, University of Rome Tor Vergata
Via del Politecnico 1, Rome 00133, Italy
ubaldo.cella@uniroma2.it, biancolini@ing.uniroma2.it

Key words: Polymeric Heart valve, 3D printing, Computational Methods, RBF, Mock Loop

Abstract. Heart valve diseases are among the leading causes of cardiac failure around the globe. Current advances in imaging technology, in numerical simulation and in additive manufacturing are opening new frontiers in the field of development of new personalised prosthetic devices. The 3D printing technique could allow the realisation of personalised models for each patient undergoing valve replacement surgery. A CAD model of an aortic valve prosthesis was designed on the basis of elliptic-hyperboloid formulation. The resulting CAD model was used both to perform numerical in-silico simulation and to design a modular mould for AV fabrication. Simulations were performed through a novel hybrid approach based on RBF mesh morphing technique and CFD simulations. The polymeric aortic valve was manufactured by 3D printed process and spray deposition technique. To assess the in-vitro valve properties, the prototype was inserted in a custom mock circulatory loop to reproduce the aortic flow conditions. The manufacturing process of both the mould and the valve was successful and the in-vitro testing showed an effective orifice area (2.5 mm^2) and regurgitation fraction (5%) in accordance with the ISO-5840-2. The novel simulation strategies have revealed to be a promising approach to test both structural and functional device performances.

1 INTRODUCTION

The heart valves play a crucial role in regulating the blood flow by continuous cyclic opening and closing under an extremely demanding mechanical environment. In case of valve pathologies, prosthetic heart valves have been commonly used to address the increasing prevalence of valvular heart disease. The ideal prosthetic heart valve replacement should closely mimic the characteristics of a normal native heart valve. Currently, available options for heart valve replacement include mechanical (MHV) and bio-prosthetic (BHV) valves, both of which have severe limitations [1]. The long-term durability is the main advantage of MHVs, but their use is limited by substantial risks of thrombogenicity. Involving the use of 3D printed mechanical valves exhibited a thrombogenicity potential index comparable with the BHVs score and, consequently, much lower if compared with other MHVs [2]. BHVs do not show thrombogenicity complications and circumvent the problem of anti-coagulation medications. Moreover, they have significantly improved hemodynamic results, lower gradients and larger AV/orifice areas [3]. To date, pericardium xenografts are the only leaflet material for flexible prosthetic AV to gain FDA and CE approval. However, many of the persistent limitations associated with bioprosthetic valves are inherently related to the tissue material (i.e. calcific degeneration, crimping and deployment damage, durability). Polymers provide better design freedom to overcome many of the aforementioned limitations as they offer the possibility to specifically design and optimize a valve from the bottom up, and can be potentially produced with high reproducibility and lower costs [4]. Despite the numerous advantages of BHVs, they are not as mechanically robust if compared to MHVs and they exhibit limited durability in younger patients (particularly those younger than 60 years), which is a current obstacle hindering the progress of bioprostheses. Polymers provide better design freedom to overcome many of the aforementioned limitations. In recent years, significant advances have been made in the world of polymeric materials and subsequently novel polymeric AV have been developed, showing very promising in-vitro results [5,6]. In-silico characterization plays a key role within the context of development of new AV designs. The in-silico evaluation of prosthetic heart valves can be divided in structural simulations, where the fluid flow across the prosthetic valve is neglected and only the pressures is considered as a condition of the structure domain [7,8], and fluid-structure interaction (FSI) simulations, where the interaction between two different physics phenomena, mechanical and fluid dynamic, computed in separate analyses, are taken into account [9,10]. The structural simulation of the valve opening presents the major drawback of overestimating the deformations as the pressures are applied uniformly on the leaflet during the whole opening phase, while in the FSI simulation the load conditions depend directly on the leaflets opening position [11,12]. A negative aspect of FSI simulation concerns a significant increase in computing time.

In the current study, we present a complete design of a novel polymeric AV for surgical application, from numerical hemodynamic evaluation to valve manufacturing based on 3D printing technique and hydrodynamic in-vitro test. In particular a novel combined approach of structural simulations, morphing techniques and CFD simulations is presented to simulate the opening phase of the valve. Regarding the mesh morphing techniques, the theoretical basis of RBF was

established [13–16] to manage problems of multidimensional interpolation. These approaches has been demonstrated to be useful for the study of hemodynamic CFD problems [17, 18].

2 MATERIALS AND METHODS

Our study consists of four main blocks: valve design (i), numerical simulation (ii), valve manufacturing (iii) and experimental tests (iv). The entire scheme of the study is reported in Figure 1.

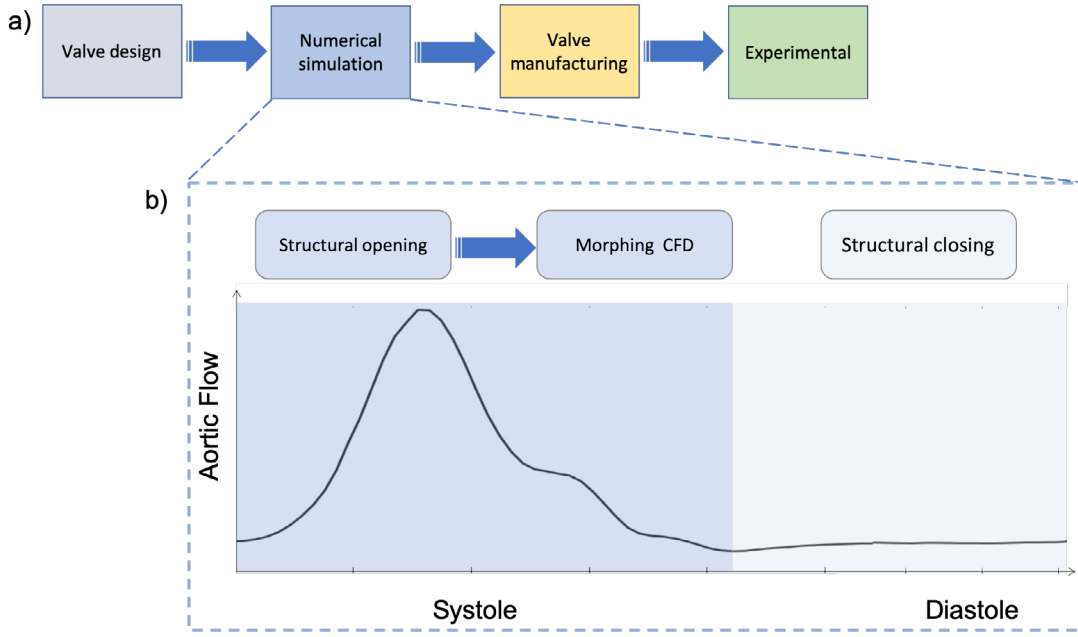


Figure 1: Overall workflow of the study (a) and schematic workflow of the numeral approach.

Valve design - The polymeric AV prosthesis is composed of three leaflet attached to a polymeric crown shape ring. The ring has the function to support the leaflets during their opening and closing phases and to constrain the valve on the aortic root. A tri-leaflet geometry permits to reproduce the kinematic of the replaced native AV. In this study the leaflet shape in the close position was defined by the elliptic hyperbolic surface [19] as described in the following equation:

$$\frac{x^2}{a^2} + \frac{y^2}{b^2} - \frac{z^2}{c^2} = -1 \quad (1)$$

where x, y, z are the spatial coordinates of the surface and a, b, c are the surface shape parameters. In particular the fraction c/a represents the slope of hyperbola curve asymptotes; its value was assumed equal to $\pm\sqrt{3}/3$ in order to realize two hyperbola asymptotes with an angle of 120° [20]. In this condition two adjacent leaflet approach the common asymptote at the commissure zone of the valve, leaving theoretically no gap between them. A small gap was left

at the commissure level in order to avoid cuspid zones. The complete 3D geometry of the valve was designed using Solidworks [®] software (Dassault Systemes, Waltham, MA).

Numerical simulations - The finite element analyses of the AV behavior during the cardiac cycle were conducted by simulating the systolic (valve opening) and the diastolic phases (valve closing) separately. In the systole phase the system is influenced by both static and dynamic pressures. On the contrary, in the diastolic phase, the velocities of the fluid flow became negligible so the system is influenced only by the static physiological transvalvular pressure.

Regarding the systolic phase a FSI simulation was performed. In particular a "1-way" FSI approach was implemented, according to the following phases: firstly a transient structural analysis was performed applying a systolic physiological pressure on the valve leaflets in the FEM model, (i); selected deformed valve shapes resulting from the FEM analysis were used to define the mesh morphing system (ii), and finally a FSI simulation was done by imposing the adaptation of the fluid domain on the basis of the leaflets position (iii), (Figure 1.b).

In the structural analysis of the AV, the model was meshed with tetrahedral elements (727000 SOLID187). The AV ring material was assumed as linear elastic isotropic with Young's modulus equal to 4.6 MPa and Poisson ratio of 0.4 [21]. Regarding the leaflet, the material properties were assumed linear elastic isotropic with Young's modulus equal to 6.5 MPa and Poisson ratio of 0.4. The AV was constrained at the lower face of its ring in order to avoid translation and rotation in all directions. The pressure load was applied on the leaflets and it was set equal to systolic physiological transvalvular pressure. The load was applied by a step time of 0.5 s, instead the solution was found by using a substep time equal to 10^{-5} s.

Three different deformed configurations were exported from the FEM simulation and used as inputs for the mesh morphing technique (Figure 2). Due to the capability of the *RBF Morph* tool, the deformed shapes were exported in stereolithographic format (.STL) and used as target for the morphing action without any additional file conversion.

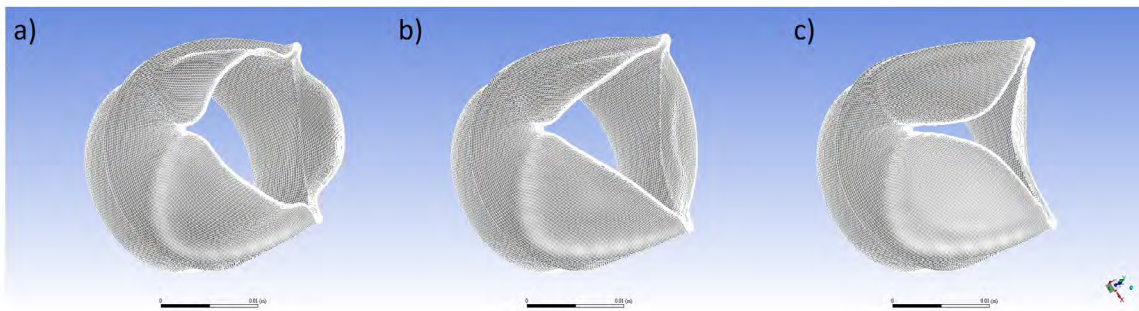


Figure 2: Example of morphing process at three different opening levels: maximum opening (a), mid opening (b), minimum opening (c).

The definition of the source points was performed interactively using a GUI and subsequently batch commands were adopted to combine the shape modifications in a non-linear fashion. The displacement of the prescribed set of source points and the combination of RBF solutions are then amplified according to the parameters that constitute the parametric space of the model

shape. The mid opening position was used as the starting baseline shape from which the mesh morphing process is performed (Figure 2.b). In our case two reference geometries were adopted to implement the RBF solution: one at a maximum opening (Figure 2.a) and one at the minimum opening (Figure 2.c). Two separated RBF solutions were setup according to the two reference target geometries. The setup split gave the possibility to cope the leaflet shape during the displacements in all positions between the two extreme configurations. The two solutions were made available to the solver to adapt the fluid domain for the subsequent CFD computation. Figure 3 displays the source points involved in the RBF setup and the visualization of the STL surface of the valve in the maximum opening position used as target for the morphing action. The RBF solution was configured to map the complete mesh morphing through an amplification parameter ranging from 0 to 1, where the value 1 corresponds to the target geometry.

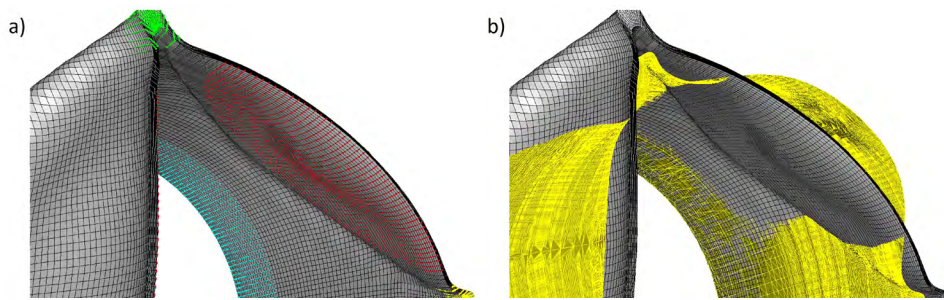


Figure 3: Setup of the RBF problem valve opening: source (a) and target points (b).

The CFD consisted in a pressure based transient run, in which the Realizable $k - \epsilon$ turbulence model was adopted. The boundary layer was solved by using standard wall functions. The fluid was considered as incompressible and non-Newtonian, the viscosity was modeled through the Carreau formulation. The analysis for the systolic phase was extended up to 0.5 seconds with a time step of 0.005 seconds. To correctly control the fluid domain modification through the morphing action on the mesh, a custom *Scheme* script was continuously recalled at every time step. The implemented procedure was in charge of loading the opportune RBF solution (depending on the target position with respect to the mid shape of the valve) and of amplifying it by a value given by a sinusoidal law with the computation time. The minimum opening position occurred at the beginning and at the end of the computation while the maximum opening occurred at 0.25 seconds. A custom UDF (User Defined Function), written in *C* language, was used to define the velocity inlet and pressure outlet time history profiles to be imposed as boundaries condition.

Concerning the diastolic phase, the valve closing was simulated through a structural transient analysis. The diastolic simulation was ran with the same FEM model described in the previous structural systolic simulation. leaflets surface was loaded with a pressure equal to diastolic physiological transvalvular pressure.

The structural transient analyses were performed with software *ANSYS Mechanical*; the fluid dynamic analysis was obtained by the *ANSYS Fluent* CFD solver and the *RBF Morph* tool [15] was used for mesh morphing techniques, which is recognized to constitute one of the most efficient mathematical frameworks to face the morphing problem [22].

Valve manufacturing - The valve leaflets were fabricated using spray technology and a custom 3D printed mould-modular outer mould system. The thermoplastic silicone polycarbonate urethane (Carbosil) was supplied by DSM Biomedical (Geleen, The Netherlands) for valve leaflets manufacturing. The valve ring was made by fused deposition technique, using a CarboSil extruded filament, according to [21]. The fabricated valve ring was positioned onto a tubular mould and dipped in a CarboSil 10% - tetrahydrofuran/dioxane 1:1 solution for 10 times. A 2% CarboSil solution containing 30% of silicone (polydimethylsiloxane, PDMS) was sprayed onto the mould by a custom spray-machine apparatus (Figure 4 (a)), allowing the polymer deposition in microfibrillar structure on the basis of the phase-inversion principle [23]. The spray process fabrication parameters were the following: 400 cycles, flow rate of 2 ml/min and rotation speed of 88 RPM. The mould with the sprayed polymer was dipped again in CarboSil solution for 10 times. Finally, the 3-layered tubular valve was housed in a valve mould, pressed by a modular outer mould (Figure 4 (b)) and incubated in distilled water at 40°C o.n. to allow the valve consolidation. The material excess on the leaflets was removed by a welder at 110°C. The polymeric valve was stored in distilled water up to hydrodynamic characterization (Figure 4 (c)).

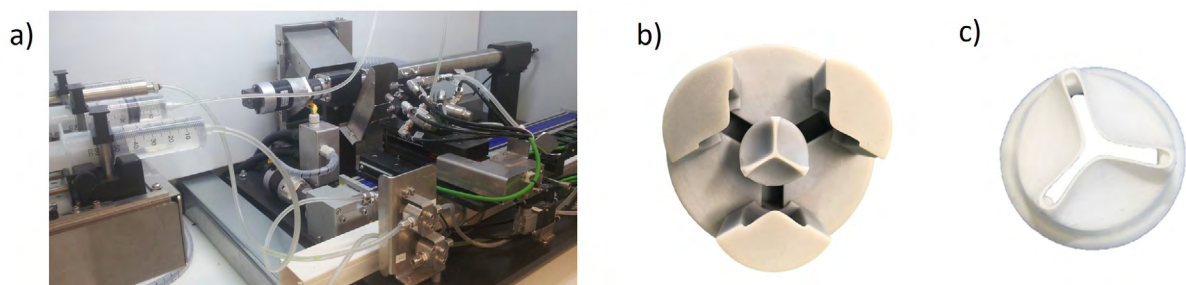


Figure 4: Spray machine (a); custom mould/modular outer mould system (b) and final valve (c).

In vitro tests - The hydrodynamic performances of the polymeric HV were evaluated by following the directives of ISO-5840 standard. In particular the manufactured valve was positioned inside a custom mock circulatory loop (Figure 5) able to reproduce the left ventricle flow and pressure conditions. The setup consists in an custom alternative piston pump, able to apply mitral and aortic pulsatile flows on the mock system. To guarantee physiological pressure conditions on the aortic outlet, a pinch valve resistance and a compliant cylindrical air chamber were adopted. The atrial physiological pressure was obtained by the insertion of another pinch valve resistance and a compliant cylindrical air chamber in addition to a centrifugal pump at the piston pump inlet pipe. The HV was placed into a 3D printed seat. The valve seat was designed with two orifices to measure the transvalvular pressure during the hydrodynamic tests. The transvalvular and the ventricular pressures were measured using clinical TruWave transducers (Edwards, Irvine, California, USA) A clamp-on ultrasound flow sensor was placed at the piston pump outlet to evaluate the resulting aortic flow. The device hydrodynamic testing was per-

formed with heart-rate of 70 bpm, cardiac output of 5 L/min (with flow systolic peak equal to 35 l/min), mean aortic pressure of 100 mmHg and aortic peak systolic pressure 120 mmHg. To define the valve performances minimum tele-diastolic, maximum systolic, the transvalvular drop pressures were evaluated to calculate the Effective Orifice Area (EOA) and the total regurgitation fraction (RF) parameters.

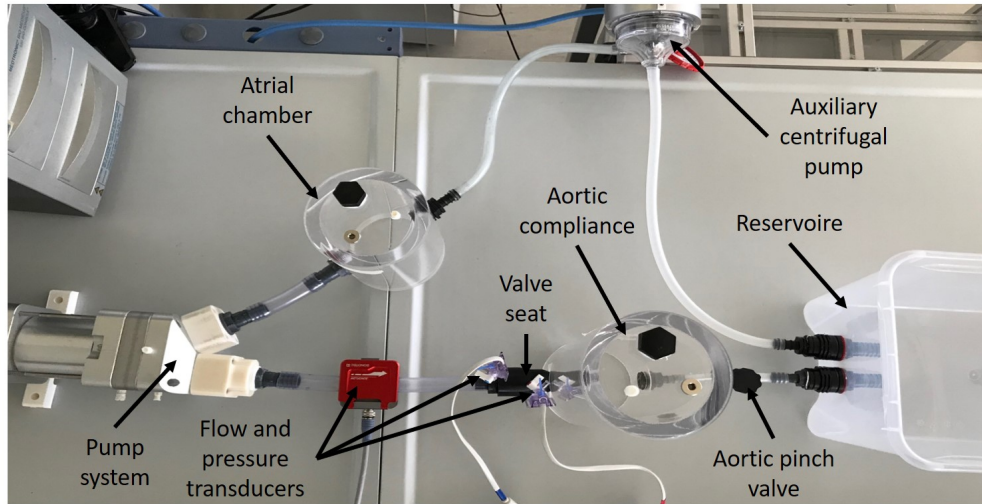


Figure 5: Mock circulatory loop

3 RESULTS

Numerical simulations - The structural simulation of the valve opening and closing phases are reported in Figure 6. During the opening phase the maximum radial displacement of the leaflet was equal to 8.4 mm (Figure 6.a) and the maximum equivalent Von-Mises strain value was equal to 0.6 mm/mm (Figure 6.b). Regarding the closing phase, the maximum radial contraction of the leaflet was equal to 3.8 mm (Figure 6.a) and the maximum equivalent Von-Mises strain value was equal to 0.20 mm/mm (Figure 6.b).

From the CFD simulations the pressure and velocity fields during the valve opening and closing can be observed in Figure 7 and Figure 8, respectively. In the acceleration phase, it was possible to observe a uniform pressure distribution on both the external and internal leaflet surfaces (Figure 7.a). On the contrary, a pressure gradient was visible on the internal surface of the leaflet during the peak systolic phase (Figure 7.b).

In vitro tests - Figure 9 shows a representative example of the pressure and flow trends measured during the in-vitro test. The reported values were consistent with typical systemic in-vivo waveforms. In particular, the aortic pressure was in the 125/80 mmHg range, ventricular pressure was in the 130/0 mmHg range, while the aortic output was 5 l/min with a peak equal to 35 l/min. The corresponding EOA and RF values were 2.5 cm^2 and 5%.

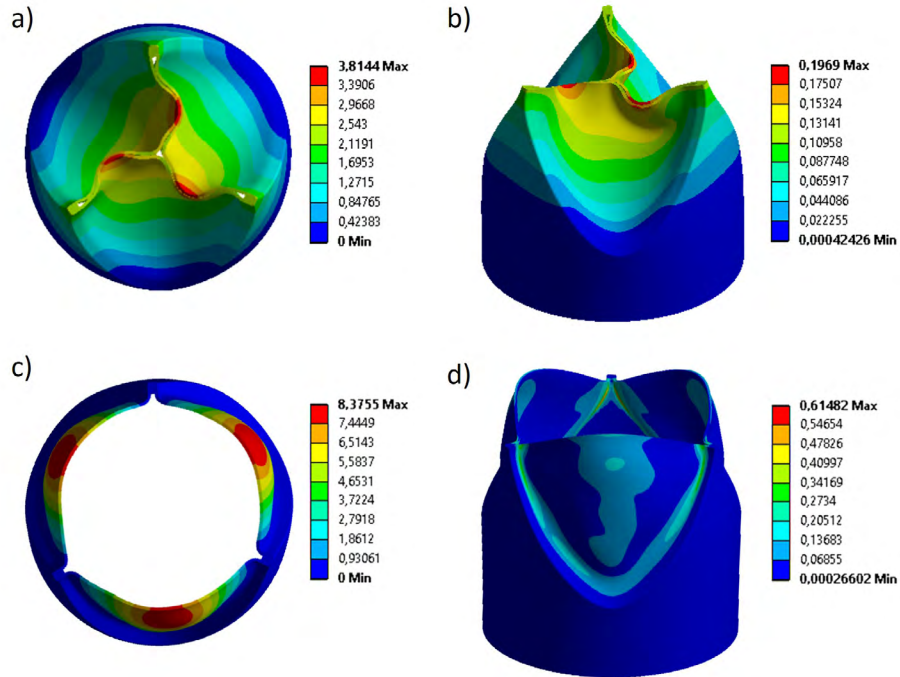


Figure 6: Systole results a) radial displacement (mm) and b) equivalent strain (mm/mm); diastole results c) radial displacement (mm) and d) equivalent strain (mm/mm)

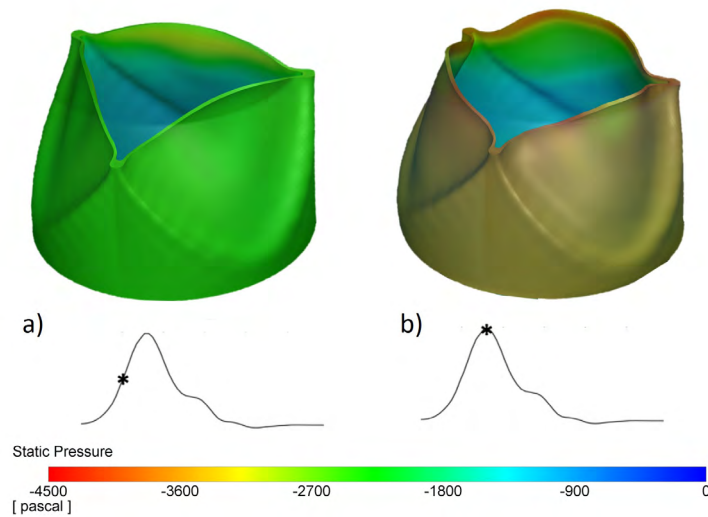


Figure 7: Pressure fields at two instances throughout the cardiac cycle corresponds to the acceleration phase (a) and to peak systole (b).

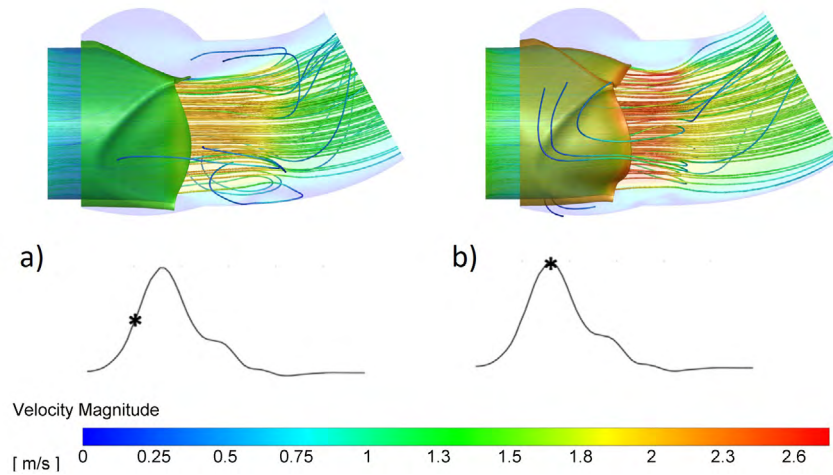


Figure 8: Flow velocity streamlines at two instances throughout the cardiac cycle corresponds to the acceleration phase (a) and to peak systole (b).

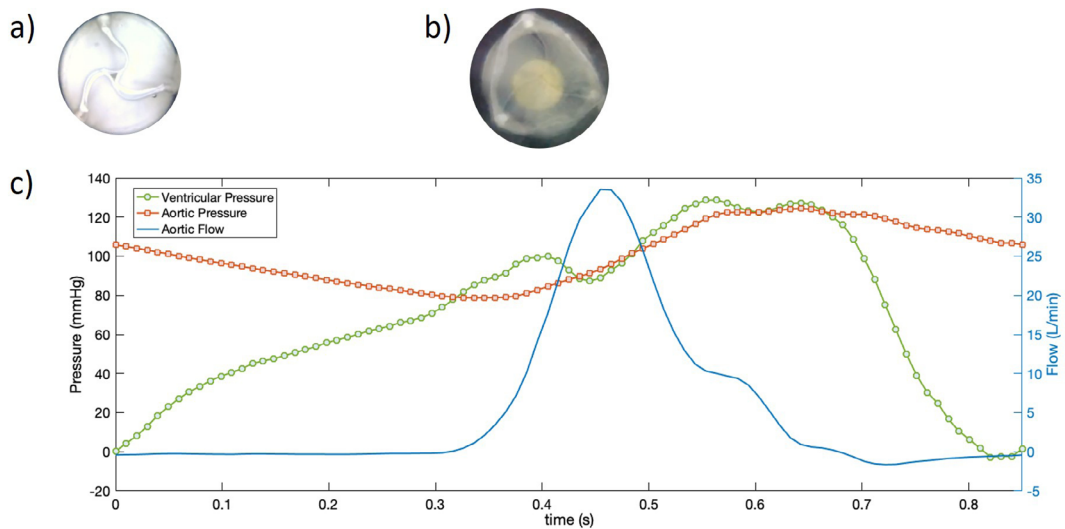


Figure 9: Example of valve closure (a); valve opening (b) and circuit transvalvular pressures and aortic flow (c).

4 DISCUSSION AND CONCLUSIONS

In this paper, the feasibility of a custom polymeric surgical AV prosthesis was demonstrated. The structural simulation of the AV opening/closure process was successful. The reported maximum strain was lower than the corresponding ultimate strain value of the material (4.73 mm/mm according to the value reported by DSM material datasheet for Carbosil). The simulations of the valve during the cardiac cycle presented in this paper exhibited an overestimation of the

leaflets displacement as a consequence of the uniform pressure load conditions. Nevertheless, the proposed approach correctly reproduced the AV opening kinematics that were successfully transferred to the CFD analysis through the morphing technique. A given advantage of adopting the morphing technique is constituted by the possibility to obtain a CFD evaluation of the AV without the computational burden of classic FSI analysis. The developed workflow represents a preparatory step that allowed to lay the basis of the development of a complete 2-way FSI setup based on mesh morphing method.

The manufacturing process based on 3D printing and spray technologies made possible the realization of a full functional valve. These manufacturing approaches represent a valid alternative to the traditional fabrication valve process, based on injection moulding [20] and dip coating [24] techniques. Moreover, it is important to underline the possibility to open new pathways in the world of personalized medicine. In particular, versatility of 3D printing technique allows an high customization of the valve prosthesis in terms of patient specific dimensions and sizes.

Concerning the in-vitro results, a complete hydrodynamic setup for the prosthesis validation has been correctly developed. The performance of the manufactured device were confirmed on the basis of the ISO5840-2. In particular, the EOA and the RF indexes showed values within the reported standard ranges ($EOA > 1.95 \text{ cm}^2$ and $RF < 20\%$). To obtain a further characterization of the device, future works will include a full fatigue fluid-dynamic validation test for both the Carbosil and the AV prosthesis. Different studies concerning the development of AV prostheses reported thrombogenicity evaluation [25], this aspect represents another possible point of improvement of the current work. Nevertheless, it is worth to affirm that the preliminary fluid dynamic parameters reported are promising and remarkable.

ACKNOWLEDGEMENTS

This work was supported by the VIVIR (PE-2013-02357974) grant from the Minister of Health and by 3D VIRTUAL BABY HEART project (GR-2016-02365072).

REFERENCES

- [1] Deon Bezuidenhout et al. Polymeric heart valves for surgical implantation, catheter-based technologies and heart assist devices. *Biomaterials*, 36:6 – 25, 2015.
- [2] Lawrence Scotten. Are anticoagulant independent mechanical valves within reach-fast prototype fabrication and in vitro testing of innovative bi-leaflet valve models. *Ann Transl Med*, 3(14):197–197, August 2015.
- [3] Marie-Annick Clavel et al. Comparison of the hemodynamic performance of percutaneous and surgical bioprostheses for the treatment of severe aortic stenosis. *Journal of the American College of Cardiology*, 53(20):1883–1891, 2009.
- [4] Kan Yan Chloe Li. Bioprosthetic heart valves: Upgrading a 50-year old technology. *Front.Card. Medicine*, 6, 2019.

- [5] Oren Rotman, Brandon Kovarovic, et al. Novel polymeric valve for transcatheter aortic valve replacement applications: In vitro hemodynamic study. *Annals of Biomedical Engineering*, 47, 09 2018.
- [6] Benyamin Rahmani, S Tzamtzis, et al. In vitro hydrodynamic assessment of a new transcatheter heart valve concept (the triskele). *Journal of cardiovascular translational research*, 10, 12 2016.
- [7] Qing Wang and Shiwen Chen. A general class of linearly extrapolated variance estimators. *Statistics Probability Letters*, 98:29 – 38, 2015.
- [8] Simone Morganti, Michele Conti, et al. Simulation of transcatheter aortic valve implantation through patient-specific finite element analysis: Two clinical cases. *Journal of Biomechanics*, 47(11):2547 – 2555, 2014.
- [9] Ram Ghosh, Gil Marom, et al. Comparative fluid-structure interaction analysis of polymeric transcatheter and surgical aortic valves' hemodynamics and structural mechanics. *J. Biomech. Eng.*, 140, 06 2018.
- [10] Giulia Luraghi, Wei Wu, Francesco De Gaetano, et al. Evaluation of an aortic valve prosthesis: Fluid-structure interaction or structural simulation? *Journal of Biomechanics*, 58:45 – 51, 2017.
- [11] Giulia Luraghi and Francesco others Migliavacca. Study on the accuracy of structural and fsi heart valves simulations. *Cardiovascular Engineering and Technology*, 9, 08 2018.
- [12] Finja Borowski, Michael Smann, and othersl. Fluid-structure interaction of heart valve dynamics in comparison to finite-element analysis. *Current Directions in Biomedical Engineering*, 4:259–262, 09 2018.
- [13] Yong Duan. Duan, y.: A note on the meshless method using radial basis functions. *comput. math. appl.* 55(1), 66-75. *Computers Mathematics with Applications*, 55:66–75, 01 2008.
- [14] Ubaldo Cella, Corrado Groth, et al. Geometric parameterization strategies for shape optimization using rbf mesh morphing. *Lecture Notes in Mechanical Engineering*, pages 537–545, 01 2017.
- [15] M.E. Biancolini, C. Biancolini, E. Costa, D. Gattamelata, and P.P. Valentini. Industrial application of the meshless morpher RBF morph to a motorbike windshield optimisation. In *4th Eu. Aut. Sim. Conf.*, Munich, Germany, 2009.
- [16] Marco Evangelos Biancolini. *Fast radial basis functions for engineering applications*. 2018.
- [17] K. Capellini et al. Computational fluid dynamic study for ataa hemodynamics: An integrated image-based and radial basis functions mesh morphing approach. *J Biomech Eng*, 140(140):111007–111017, 2017.

- [18] K. Capellini et al. A coupled cfd and rbf mesh morphing technique as surrogate for one-way fsi study. 2019.
- [19] M.E.Leat and J.Fisher. A synthetic leaflet heart valve with improved opening characteristics. *Medical Eng Physics*, 16(6):470 – 476, 1994.
- [20] Hongjun Jiang, Gord Campbell, et al. Design and manufacture of a polyvinyl alcohol (pva) cryogel tri-leaflet heart valve prosthesis. *Medical Engineering Physics*, 26(4):269 – 277, 2004.
- [21] Emanuele Gasparotti et al. A 3d printed melt-compounded antibiotic loaded thermoplastic polyurethane heart valve ring design: an integrated framework of experimental material tests and numerical simulations. *Int. J. Poly. Mat.Polymeric Biomat.*, 68(1-3):1–10, 2019.
- [22] Stefan Jakobsson and Olivier Amoignon. Mesh deformation using radial basis functions for gradient-based aerodynamic shape optimization. *Computers & Fluids*, 36(6):1119–1136, 2007.
- [23] E Briganti, Paola Losi, et al. Silicone based polyurethane materials: A promising biocompatible elastomeric formulation for cardiovascular applications. *Journal of materials science. Materials in medicine*, 17:259–66, 2006.
- [24] New polyurethane heart valve prosthesis: design, manufacture and evaluation. *Biomaterials*, 17(19):1857 – 1863, 1996.
- [25] Hemodynamic and thrombogenic analysis of a trileaflet polymeric valve using a fluid-structure interaction approach. *Journal of Biomechanics*, 48(13):3641 – 3649, 2015.